

## IDENTIFICATION OF LipY INHIBITORS AS ANTITUBERCULAR AGENTS USING STEPWISE VIRTUAL SCREENING

Suresh Satpati<sup>1</sup>, Parameswari Behera<sup>2</sup> and Anshuman Dixit<sup>1\*</sup>

<sup>1</sup>Department of Translational Research and Technology Development, Drug Design and Discovery Division, Computational biology and bioinformatics lab, Institute of Life Sciences, Bhubaneswar-751023, Odisha, India.

<sup>2</sup>Dept. of Bioinformatics, Center for Post Graduate Studies, Orissa University of Agriculture and Technology, Bhubaneswar- 751003, Odisha, India.

### ABSTRACT

The LipY enzyme is a 437 amino acid protein that belongs to hormone-sensitive lipase family and a sub member of PE-PGRS (Pro-Glu - polymorphic CG-repetitive sequences) family of proteins. The LipY function helps in survival and functioning of *Mycobacterium tuberculosis* and has been recognized as a target to prevent *Mycobacterium tuberculosis* infection. The degradation of triacylglycerol (TAG) helps in sustainability of LipY protein during dormant stage. It is the key receptor protein present in *Mycobacterium tuberculosis*. This catalytic feature of LipY enzyme protein was recognized as better target to prevent an individual from *Mycobacterium tuberculosis* infection. Since, no crystal structure is available in different protein databases. We have started our investigation by following systematic approach i.e. homology modeling, compound screening and molecular docking. The aim of this study is to screen out the molecules that have higher affinity to bind with residues present in LipY active site. In the current work, we report a systemic virtual screening for inhibitors of LipY using computational approaches viz. homology modeling, shape based screening, molecular docking and fingerprint based clustering. We have identified some compounds that have shown good binding with LipY active site. The identified compounds were clustered to identify diverse leads.

**Keywords:** Tuberculosis, LipY, Ligand supported homology modelling, MM/GBSA.

### INTRODUCTION

Tuberculosis (TB) is an airborne infectious disease caused by the rod-shaped pathogen *Mycobacterium tuberculosis*<sup>1</sup>. It is a leading cause of death worldwide despite being known since antiquity. An estimated 9 million people fell sick, and 1.5 million died due to TB in 2013<sup>2,3</sup>. A major cause of high TB mortality rate is the emergence of multidrug-resistant TB (MDR-TB) and extensively drug resistant TB (XDR-TB)<sup>4</sup>. The cell wall of *Mycobacterium tuberculosis* is highly complex with the majority of the composition is lipid that controls the permeability and protectiveness of the mycobacterial cell surface<sup>5,6</sup>. The cell wall does not permit many compounds to enter inside the cell that is a unique characteristic of this bacteria and is an important defense mechanism against chemical

agents<sup>7,8</sup>. The infection caused by *Mycobacterium tuberculosis* in the inner lung is known as pulmonary tuberculosis. The pulmonary tuberculosis infection may in turn affect other parts of the body like kidney, brain & liver and termed as extra-pulmonary tuberculosis that accounts for about 15-20% tuberculosis infections reported worldwide<sup>9,10</sup>. Prior to the spread of infection, the *Mycobacterium tuberculosis* stays in the latent phase. In this stage, bacteria stay dormant in the body tissues without harming the host system. However, later it may start growing and cause TB<sup>11,12</sup>.

Despite over a century of research, about one-third of the world's population is infected with TB and there are only a few drugs available for the treatment of TB<sup>13,14</sup>. In spite of the widespread use

of attenuated live vaccine and several antibiotics, the number of TB patients is still increasing<sup>151</sup> Factors like a long period of treatment, poor patient's compliance and the emergence of the drug resistant forms have contributed in making TB a global epidemic<sup>1, 16, 17</sup>. Therefore new therapeutics, with novel mechanism of action, are urgently needed to tackle this problem<sup>18</sup>.

It has been shown that two novel familial proteins i.e. PE (proline-glutamic acid) and PPE (proline-proline-glutamic acid) constitute about 10% of *Mycobacterium tuberculosis* proteome<sup>19, 20</sup>. The N-terminal domains of these PE and PPE protein families contain a large numbers of conserved proline and glutamic acid residues<sup>21</sup>

LipY, is the lipase enzyme belonging to the hormone-sensitive lipase PE family and a sub-member of PE-PGRS (Pro-Glu - polymorphic CG-repetitive sequences) family proteins present in the *Mycobacterium tuberculosis*<sup>22</sup> The presence of LipY receptor on the *Mycobacterium tuberculosis* cell surface pinpoints its essential role in interaction with host mechanisms<sup>13</sup>. The cytosol of *Mycobacterium tuberculosis* contains lipid inclusion bodies. These bodies are enriched with triacylglycerol (TAG) lipids. Under energy deprived condition, i.e. during dormant state these energy bodies are used for the survival of *Mycobacterium tuberculosis*<sup>23, 24</sup>. The LipY possesses TAG hydrolase activity that reactivates the pathogen by utilizing the stored TAG<sup>13, 24, 25</sup>. It is a key enzyme for increased virulence and immunopathogenesis of tuberculosis due to its restricted distribution in a few pathogenic species<sup>13, 25</sup>. It makes LipY an attractive target for therapeutic intervention. Strategically, the LipY target can be exploited as an important drug target against TB infection by inhibiting this reactivation process by designing new antimycobacterial compounds.

Research efforts towards the development of LipY small molecule inhibitors are currently gaining interest<sup>26, 27, 28</sup>. Recently, Saxena *et al.* have reported the identification of some new Rv3097c-encoded lipase inhibitors (LipY) that may inhibit the growth of *Mycobacterium tuberculosis* in hypoxia<sup>24</sup>. Orlistat is a potential anti-tumor agent, since this compound has only be tested on pure enzymes and in vitro on cell culture. On the contrary, Orlistat is well-known FDA-approved anti-obesity drug<sup>29, 30, 31, 32</sup>. The inhibitors reported by Saxena *et al.* were selected as starting points for the identification of new drug-like compounds to inhibit LipY.

In the current study, we have performed homology modeling, shape based screening of PubChem database and docking of the selected compounds to identify high-affinity binders of LipY. We have reported diverse compounds that can be used further for the development of effective LipY inhibitors.

## MATERIALS AND METHODS

### Active compounds dataset

A set of reported compounds (total twelve) active against *Mycobacterium tuberculosis* LipY were selected for the current study<sup>24</sup>. All the compounds were sketched and geometry optimized by minimization up to a gradient of 0.001kcal/mol using OPLS2005 forcefield<sup>33</sup>. The so prepared 3D structures were used for further studies (figure 1).

### Homology modeling of LipY protein

The LipY is a 437 amino acids length protein. Since, there is no three-dimensional crystal structure is available for LipY, a 3D homology model was prepared for the purpose of the studies. The LipY protein sequence (ID: Rv3097c) was obtained from *Mycobacterium tuberculosis* database (<http://tuberculist.epfl.ch>). The BLAST<sup>34</sup> search of LipY sequence against protein data bank resulted in the identification of X-ray crystal structure of a putative esterase from *Staphylococcus aureus* at 2.01 Å resolution (PDB ID: 3D7R) as a potential template (query coverage 45% and identity 28%). The sequence alignment was done by PROMALS3D<sup>35</sup> server using the only catalytic domain of LipY sequence and X-ray template (figure 2). PROMALS3D performs progressive multiple sequence alignment on the basis of sequence alignment, 3D constraints and available secondary structural homologs of protein. The LipY sequence was aligned with the four selected species that came from protein BLAST hit against Protein data bank database (PDB). These species namely *Archaeoglobus fulgidus*, *Pyrobaculum calidifontis*, *Staphylococcus aureus*, *Escherichia coli* alignment with the LipY sequence shown in supplementary figure 1. The homology modeling was performed by using Modeller v9.13 software<sup>36</sup> The Modeller builds homology models using satisfaction of spatial restraints. The generated models are then ranked by a probability density function (pdf). The pdf score is calculated by the stereochemical quality and satisfaction of restraints. A total of fifty models were generated and the best model was chosen on the basis of lowest pdf score as implied in Modeller 9.13. The generated 3D homology model is shown in figure 3. The final modeled protein structure was further validated by using RAMPAGE<sup>37</sup>. The best model was taken to Schrodinger Prep wizard<sup>38, 39</sup>. The correct bond-orders and ionization states were assigned; terminals were capped, and heavy atoms were minimized up to 0.3 Å RMSD.

### Ligand supported refinement of homology model

Interactions between ligand and protein binding site residues are the decisive factor for ligand's activity. The correct orientation of active site residues is essential for the proper interaction

between a ligand and a receptor. In this regard, we have performed induced fit docking (IFD) where constraints were used, to optimize proper fit and interactions with conserved residues at the binding site. This strategy is expected to enable proper receptor-ligand binding interaction that is not possible in rigid docking approaches. In recent years, this approach has gained considerable interest<sup>40-42</sup>. In this step reported most active ligand (10) was selected and docked in the generated homology model using IFD module in the Maestro<sup>43</sup>. Prior to induced fit docking, the compound was prepared in LigPrep module. A docking grid was generated using a total of sixteen active site residues that line the binding pocket. These residues are Phe250, Ser248, Leu418, Trp415, Leu417, His251, Ser309, Leu385, Asp414, Ile412, His413, Asp383, Trp339, Ser337, Pro338 and Pro384. The choice of using multiple residues was done to avoid the bias which may be introduced by choosing only one atom e.g. a slight misorientation of the side chain may result in exclusion of many important residues from the docking grid. In these sixteen residues, only few residues have shown sequence conservation across the species (shown in supplementary figure 1). It is found that the residues His251, His413, Trp339, Asp383, Ile412, Trp415 are highly conserved in which both the histidine residues are identical. While, the residues namely Phe338, Ser309 and Phe84 are partially conserved. Additionally, one hydrogen bond constraint was created between the nitrogen atom of Trp339 residue and ligand compound as reported by Saxena et al. The IFD was performed by keeping other default settings and ten complexes were generated. The best-scored pose was selected as initial complex for further studies (figure 4).

#### PubChem database retrieval, pre-processing and shape based screening

The PubChem database was downloaded from the NIH website (<https://pubchem.ncbi.nlm.nih.gov>). It contains 461937 small compounds and was used for the identification of putative inhibitors in this study. Each compound in this database is identified by a unique identification number (compound ID or CID) with information on its structure and bioactivity data. The database pre-processing was done by OpenEye FILTER program ([www.eyesopen.com/filter](http://www.eyesopen.com/filter)). The filter identifies drug-like compounds in a database using several parameters e.g. topological, solubility and functional group content etc. The FILTER program was run with default filter (Filter\_drug) settings, except for the molecular weight limit that was set to 500.

A total of 167683 compounds were selected that were subjected to conformer generation using OpenEye OMEGA software<sup>44</sup>. OMEGA performs

rapid generation of conformation using incremental rotation around single bonds, flipping rings and double bonds etc. The conformers were generated using default settings except the maximum number of conformers were set as 400. The conformers were then used for the subsequent shape based screening approach using vROCS software<sup>45</sup>. Rapid Overlay of Chemical Structures (ROCS) is a shape based method in which similar compounds are identified by overlaying their volumes with query compound(s). This approach has the potential to identify novel molecular scaffolds considerably different from the original query compounds. Out of reported active compounds, four diverse compounds (1, 2, 7 & 10) were selected as representative of the actives and used for shape based screening. It is observed that all the reported compounds have similar core structures. The major difference comes with the side chains. Therefore, in these compounds three were omitted because of very less activity (6, 9 and 12). From the remaining 7 compounds we have selected four based on the diversity of the side chains. The diverse compounds were chosen to get the consensus pharmacophore and shape for the screening. These selected compounds were imported in vROCS ligand model builder to generate shape grid. The compounds were superimposed, and pharmacophoric features generated using colour forcefield in vROCS query building interface. The generated query was used to screen the generated conformers. The compounds were ranked by TanimotoCombo score as implied in ROCS.

#### Docking of the compounds

Top-ranked 10000 compounds from vROCS were docked in the active site of the LipY homology model using software Glide in standard precision (SP) mode<sup>46</sup>. The refined LipY homology model was imported into Maestro module of Schrodinger where a grid was generated using the previously docked compound (10). The docked ligands were ranked by the GlideScore as implied in Glide. A survey of literature revealed that many different cutoffs have been used for the docking score (GlideScore starting from -4.0 kCal/Mol) in the virtual screening studies. Since, we wanted to select the molecules with a good binding affinity therefore; we chose a somewhat strict cutoff. A cutoff -7.0 kcal/mol was used to select ligands for further studies.

#### Binding affinity estimation using MM/GBSA

The binding free energy estimation was done using the molecular mechanics generalized born surface area (MM/GBSA) approach. MM/GBSA is a computationally more efficient method as compared to other similar methods e.g. MM/PBSA, thermodynamic integration (TI) and free energy perturbation (FEP). MM/GBSA allows for rigorous

free energy decomposition into contributions from different groups of atoms or types of interaction.

The binding free energy ( $\Delta G$ ) between a ligand (L) and a receptor (R) in forming the complex (RL) is calculated as:

$$\Delta G = \Delta H - T\Delta S \approx \Delta E_{MM} + \Delta g_{sol} - T\Delta S$$

Where,  $\Delta E_{MM}$ ,  $\Delta g_{sol}$  and  $\Delta S$  denote the change in gas phase molecular mechanics (MM) energy, solvation free energy, and the conformational entropy upon binding respectively.

The selected docked poses (total 9812) were re-scored using MM/GBSA as implied in Schrodinger suite<sup>47</sup> using a partially flexible receptor where residue within 5 Å of the ligand were considered flexible.

### Identification of diverse scaffolds

The selected compounds were classified and clustered on the basis of their chemical diversity. The clustering of compounds was done using scaffold hunter<sup>48</sup>. The Scaffold hunter uses scaffold tree or hierarchical clustering scheme for common scaffold identification. Here, compound datasets can be imported and different fingerprints like DaylightBitFingerprinter, EStateBitFingerprinter and EstateNumericalFingerprinter can be used for clustering of compounds. The compounds with common scaffold can be grouped together and represented in the form of a tree, table, clusters or dendrogram. This mapping of chemical properties enables the user to understand the diversity and identify the representative ligand from each cluster. We have selected diverse compounds from identified hits. The flowchart of the virtual screening is shown in figure 5.

## RESULTS AND DISCUSSION

### Validation of homology based LipY model

The modeled structure of LipY consists of 8-beta strands and five alpha helices similar to the template. The modeled structure was verified for stereochemical quality using Ramachandran plot (figure 6). In the plot, ~94.7% residues were in the favoured region, 3% residues were in allowed regions and only 2.3% residues were outliers. We have validated the modeled structure using multiple criteria. The structures were superimposed and we find a negligible RMSD of 0.285 between the model and template. The placement and orientation of the side chains was indeed worked into, in the refinement stage. The overall orientation and interactions of the ligand, matches with that reported molecules by Saxena et al. It suggests that the modeled LipY structure is of good stereochemical quality and can be used for further analysis. Moreover, all the active molecules were docked in the active site of the LipY homology model. The model was able to differentiate between highly active and inactive molecules. The average MM/GBSA score for the inactive molecules was -

52.60 while that of the active molecules was -73.28. (Supplementary Table 1)

### Docking and Virtual Screening

The reported most active inhibitor (10) was used to dock in the modeled LipY protein using IFD. The best conformation was selected based on docking score and interactions with important residues. It can be seen from figure 4 that the compound settles well in the active site of LipY protein. It is making three hydrogen bonds with Ser309, Trp339 and Asp414. It is important to note that the Ser309 is the catalytic residue responsible for the nucleophilic activity of the active site in combination with His413 and Asp383 and is a part of conserved motif (GDSAG) in LipY<sup>22</sup>. The hydrophobic dichloro ring settles well in the cavity lined by residues Leu170, Phe174, Ile412, Leu417, and Leu418. The quinolone ring is sitting in a cavity lined by Trp339, Pro180, Leu181 and 182 and Thr344. The docking score for the best binding pose was found to be -8.4 kcal/mol. The overall orientation and interactions of the ligand, matches with that reported molecules by Saxena et al. The so generated conformation of the active site was used later for docking based virtual screening. The docked pose of most active ligand was grouped with other three structurally diverse compounds from the actives. These four compounds were structurally superimposed on the basis of compounds shape and 3D chemistry using vROCS tool (figure 7). The generated active ROCS shape query was used for whole PubChem database screen. Finally, the screened database consists of 10,000 compounds were docked using a hydrogen bond constraint of Trp339 and top compounds were screened out on the basis of GlideScore. It is important to note that, the residue Asp414 is not a conserved residue while Trp339 is conserved (hydrophobic position). Therefore only Trp339 was used as constraint for the docking of all compounds. The compounds with docking score of -7.0kcal/mol and better were retained. These compounds were subjected to MM/GBSA binding affinity calculation by keeping all residues flexible within a distance of 5 Å. The compounds showing binding affinity, less than -80kcal/mol were filtered out. As a result, a total of 143 compounds (~top 20%) were selected for further analysis (figure 8).

### Identification of diverse hits

In any virtual screening study, it is paramount to identify diverse hits. The advantage of having diverse hits is that if one compound fails in later stages (i.e. animal testing, pharmacokinetics) other leads can be immediately pursued. In the current study, the compounds were clustered using structural fingerprints to identify diverse hits. This approach has the potential to effectively locate the diverse scaffolds in the initial hits. The lead

compounds from each cluster representing a pool can be selected. In this analysis, fingerprints were generated for the selected 143 compounds using EStateBitFingerprinter. Compounds were then classified on the basis of their fingerprint and number of rings present in each compound. A total of forty two clusters were identified. A scaffold tree was generated showing the clustered scaffolds (figure 9). A representative compound was selected

from each cluster on the basis of high MM/GBSA binding affinity score. Thus, total forty-two diverse hits were selected. The structures and MM/GBSA binding energy estimates for these compounds, are shown in Supplementary figure 2. The docking of top five compounds based on MM/GBSA score are shown in figure 10 and Supplementary Table 2.

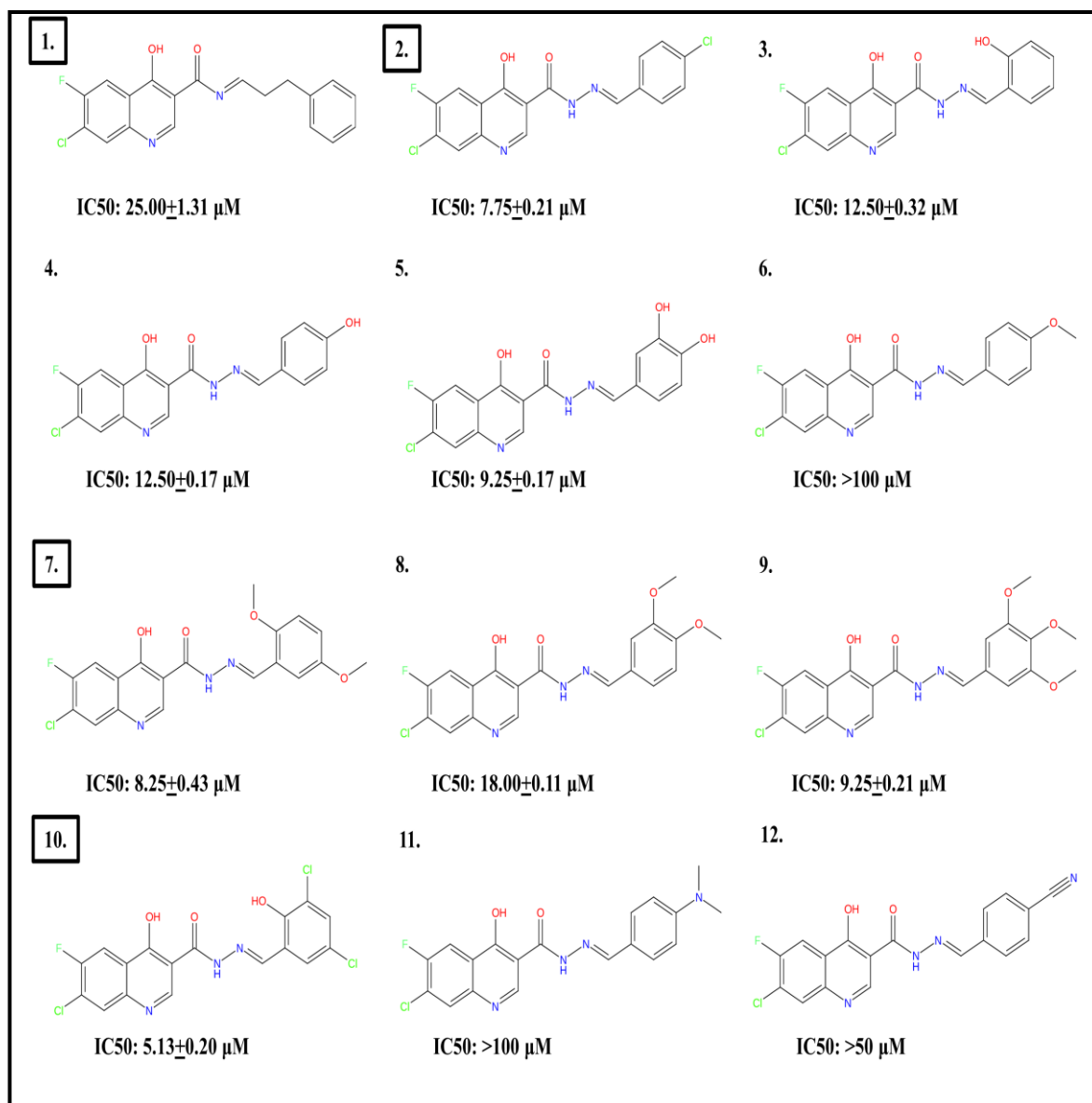


**Fig. 1: The figure depicts the 2D representation of structure and activities of reported active compounds. Where each molecule is shown with its IC<sub>50</sub> values below them. The squared black boxes indicates the four selected diverse molecules for the virtual screening**

M.tuberculosis_LipY 3d7r_chainA	169	ALETHFAIPN	NPLLALIASD	IPPLSWFLGN	-----SP	PPLINSLGQ	IVQYTTYDGM
		SVVNKYLHN	RSIMFKNDQD	VE--REFYKR	EIENRKKHKQ	PSTLN--VKA	NLEKLSLDDM
M.tuberculosis_LipY 3d7r_chainA	221	SVVQITPAHP	IQEYVVAIHG	GAFILPPSIF	HWLNYSVIAY	QTGATVQVPI	YPLVQEGGTA
		QVFRFNFRHQ	IDKKILYIHG	GFNALQSPF	HWRLLDKITL	STLYEVVLPV	YPKTPEFHID
M.tuberculosis_LipY 3d7r_chainA	281	GTVPFAMAGL	ISTQIAOHGV	SNVSVVGDSD	GGNLALAAQ	YMVSQGNPVP	SSMVLSPWL
		DT-FQAIQRV	YDQLVSEVGH	QNVVVMGDGS	GGALALSFVQ	SLLDNQOPLP	NKLYLISPIL
M.tuberculosis_LipY 3d7r_chainA	341	DV-----	-----	--GTWQISQ	AWAGNLAVND	PLVSPLYGSL	NGLPPTYVYS
		DATLSNKDTS	DALIEQDAVL	SQFGVNEIMK	KWANGLPITD	KRISPINGTI	EGLPPVYMEG
M.tuberculosis_LipY 3d7r_chainA	380	GSIDPLAQQA	VVLEHTAVVQ	GAPFSEVLAP	WQIHDWILLI	PWGL-LSWPQ	INCOGLIAA
		GGREMTHPDM	KLFEQMLQH	HOYIEFYDYP	KMVHDFPIYP	TROSHKAIKQ	IAKSIDEDV

**Fig. 2:** The sequence alignment of template (PDB ID: 3D7R) and target sequence (LipY). The colour code indicates Blue - A, L, F, I, W, V, M (hydrophobic residues), Pink - E, D (negatively charged residues), Yellow - P (Non-polar), Red - R, K (positively charged residues), Gray - G, Green - S, Q, T, N (Polar residues), Sky blue - Y, H (aromatic residues)

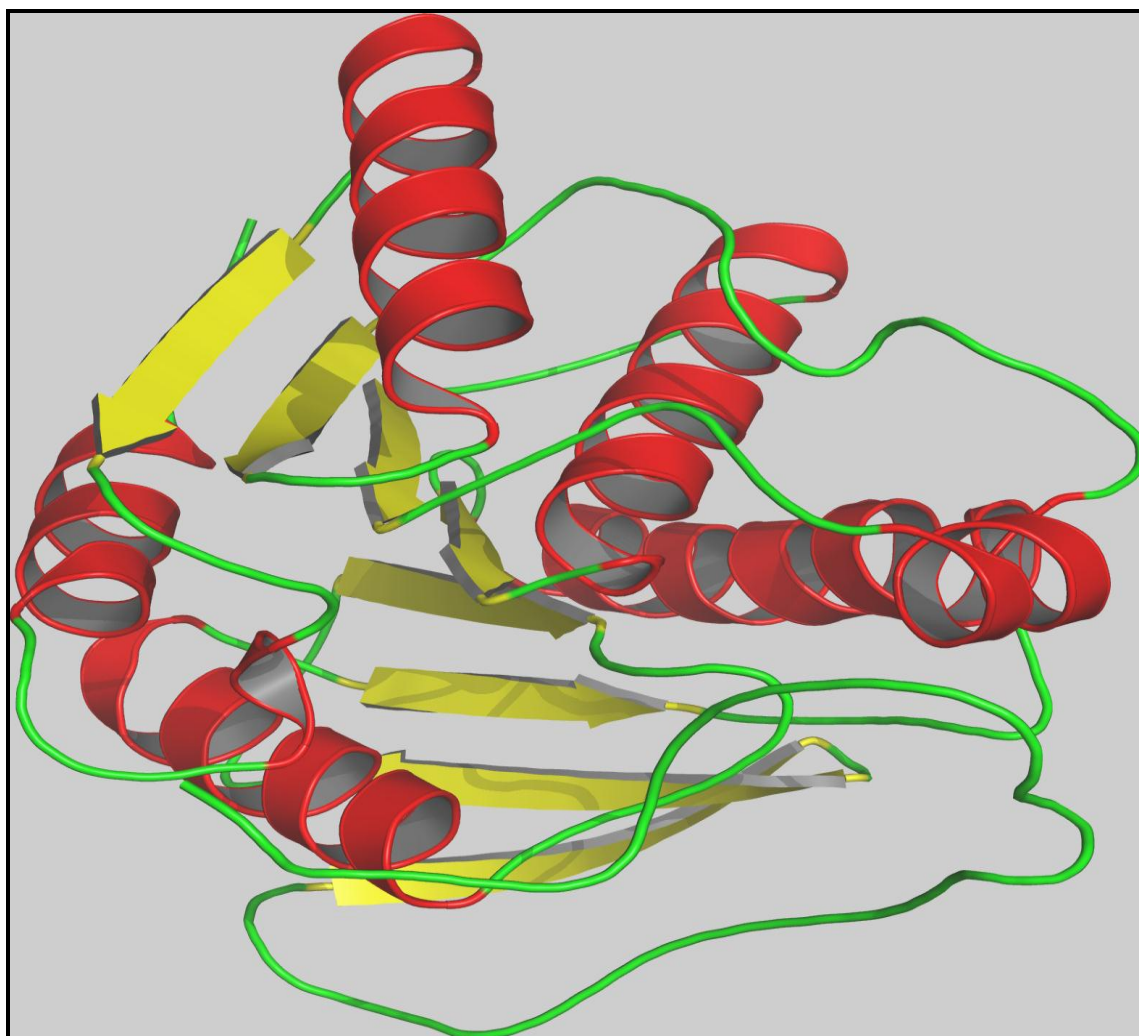


**Fig. 3:** The cartoon representation of homology modeled structure of LipY protein. The helix, sheets and loops are coloured in red, yellow and green respectively using pymol

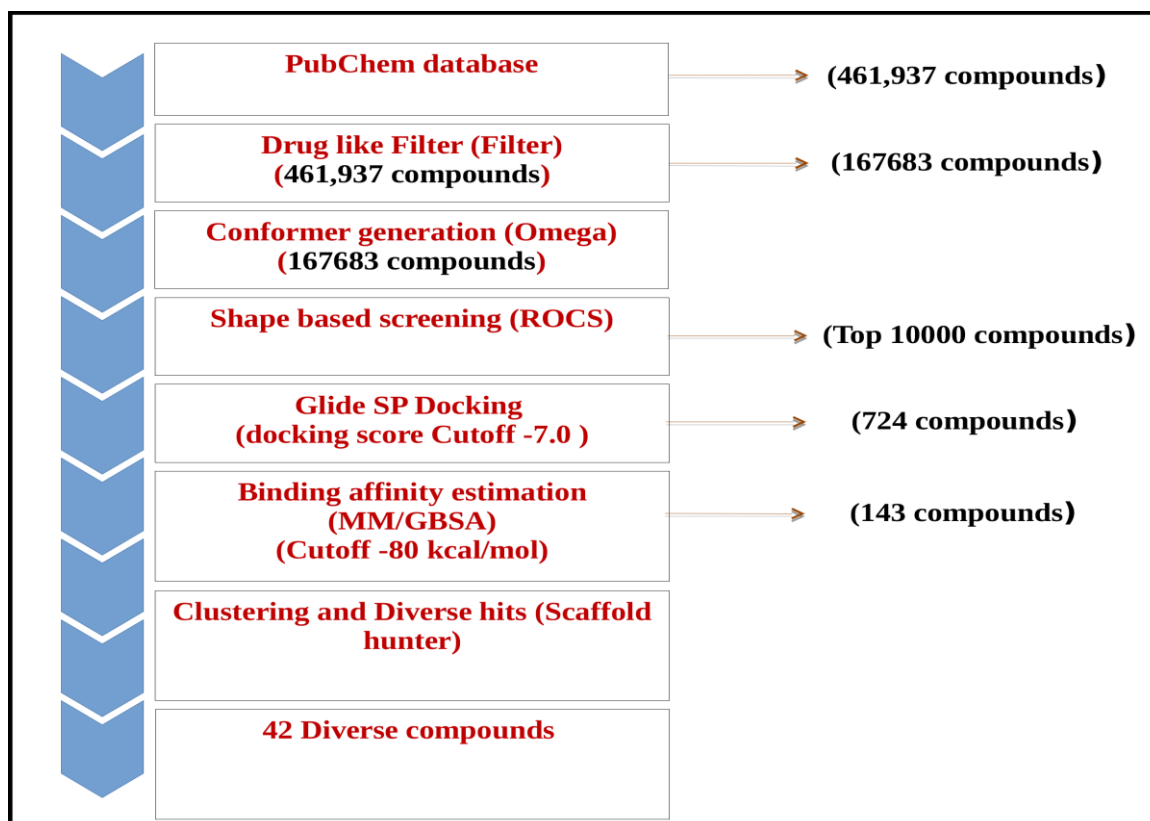


Fig. 4: The active site of the refined homology model was shown. Where, the ligand is shown in green sticks. The hydrogen bonds between ligand and active site residues are shown as pink dotted lines while active site residues are shown in white colour

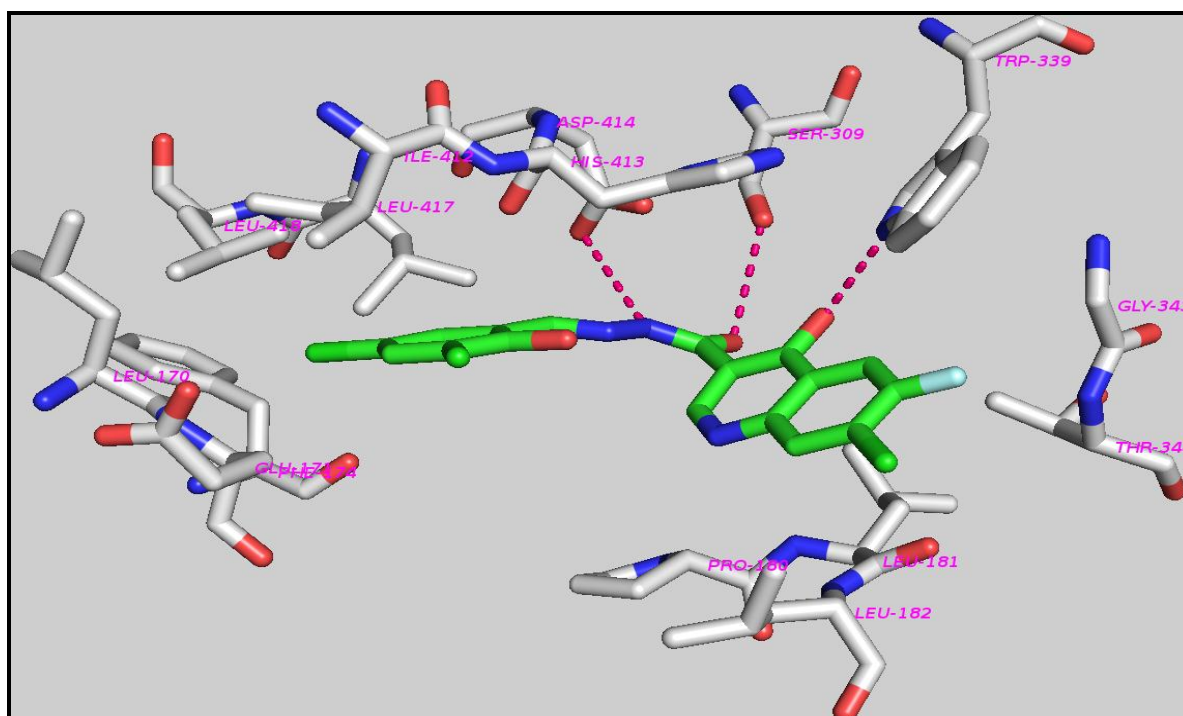


Fig. 5: The schematic representation of the overall workflow used during the entire process of docking and virtual screening of PubChem database

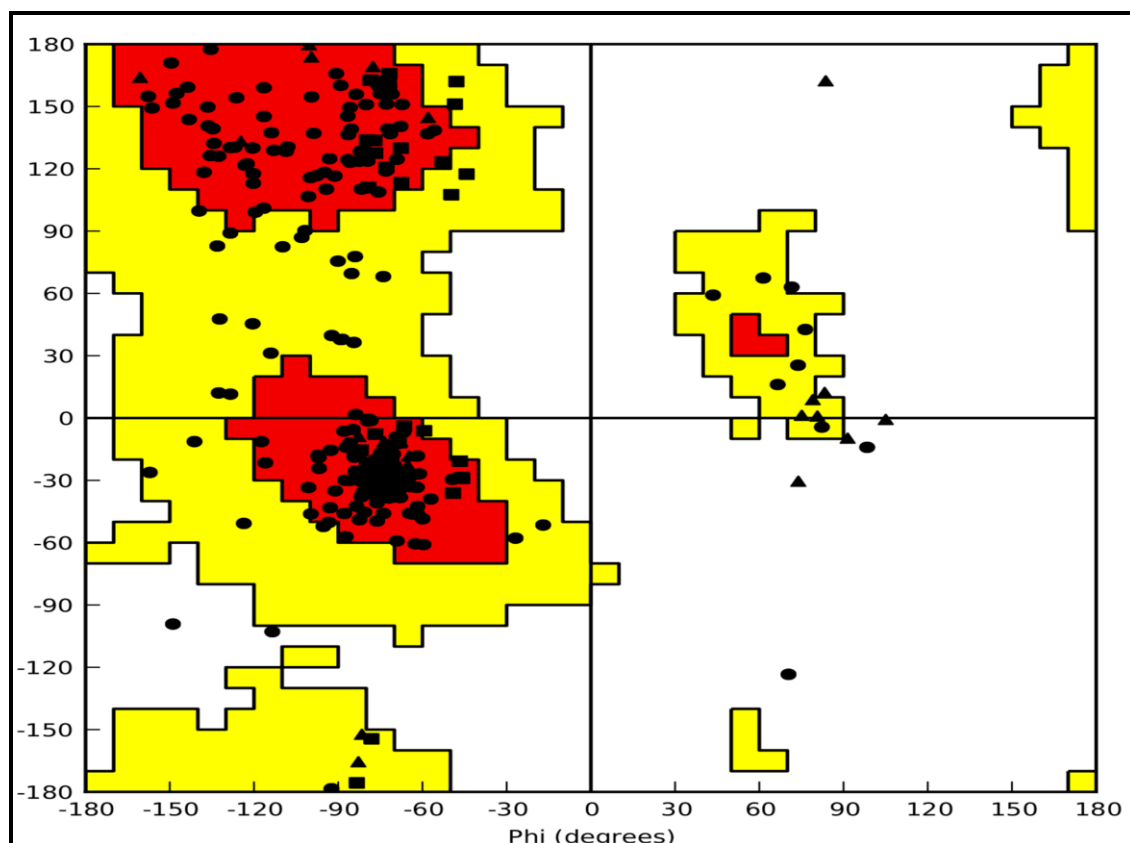


Fig. 6: The structure validation of the modeled protein for LipY target using Ramachandran plot. The residues in most favoured region (Red colour), the residues in allowed region (Yellow colour) and the residues in dis-allowed region (white colour). All residues are shown in circle except glycine in triangle

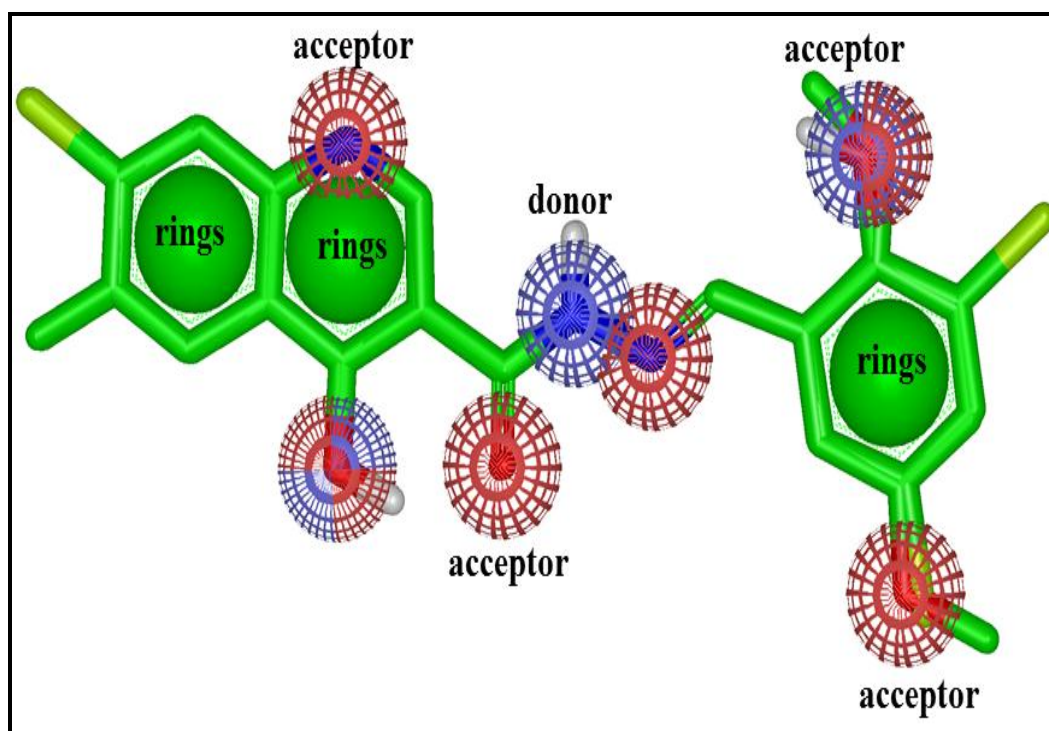


Fig. 7: The figure depicts the generated shape query using vROCS. The red and blue colour rings indicates acceptor and donor regions respectively. While, green colour indicates aromatic rings

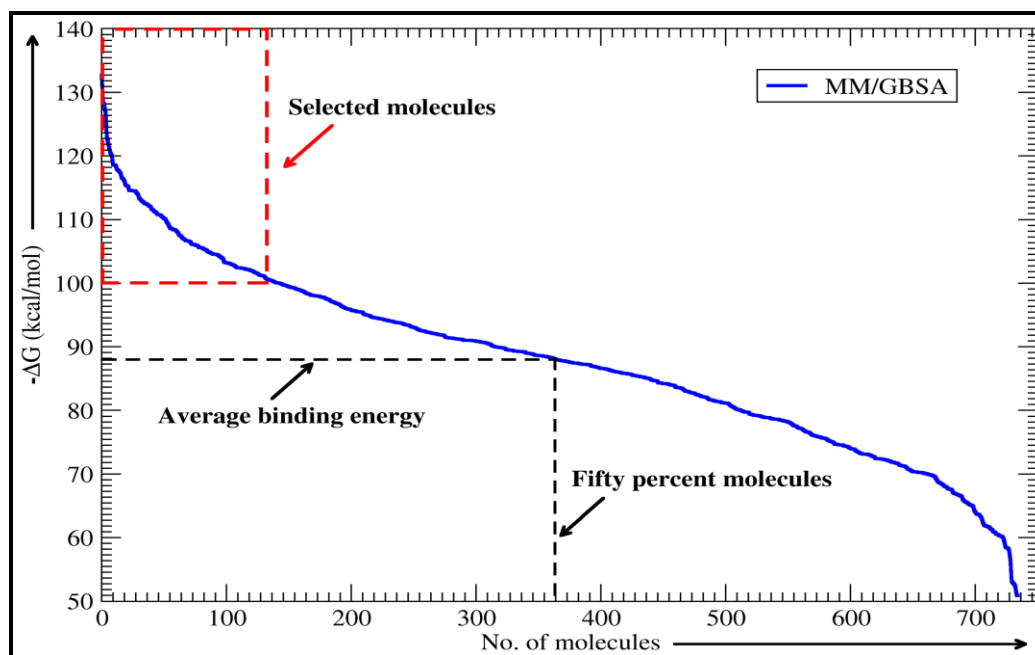


Fig. 8: The plot of MM/GBSA score vs. number of compounds. Highest scoring compounds (under red square) were selected for further analysis. The average binding energy and percentage molecules were shown in black dashed line

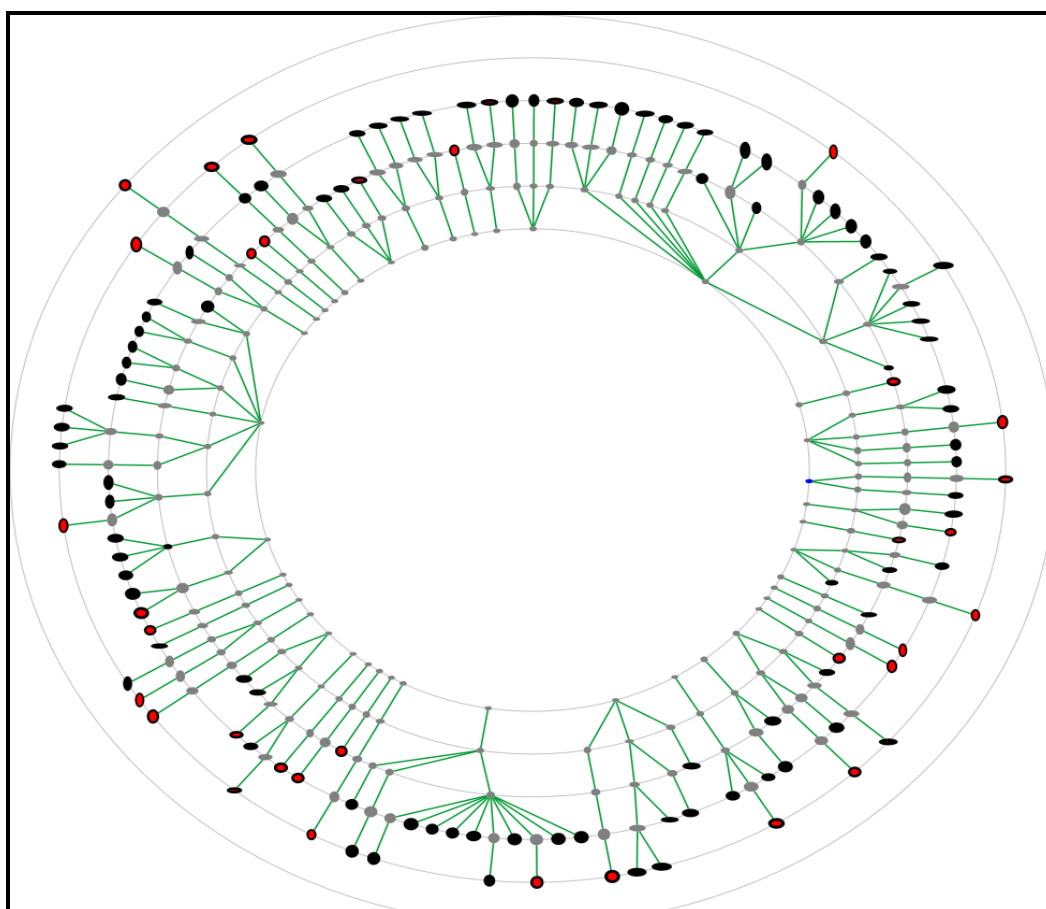
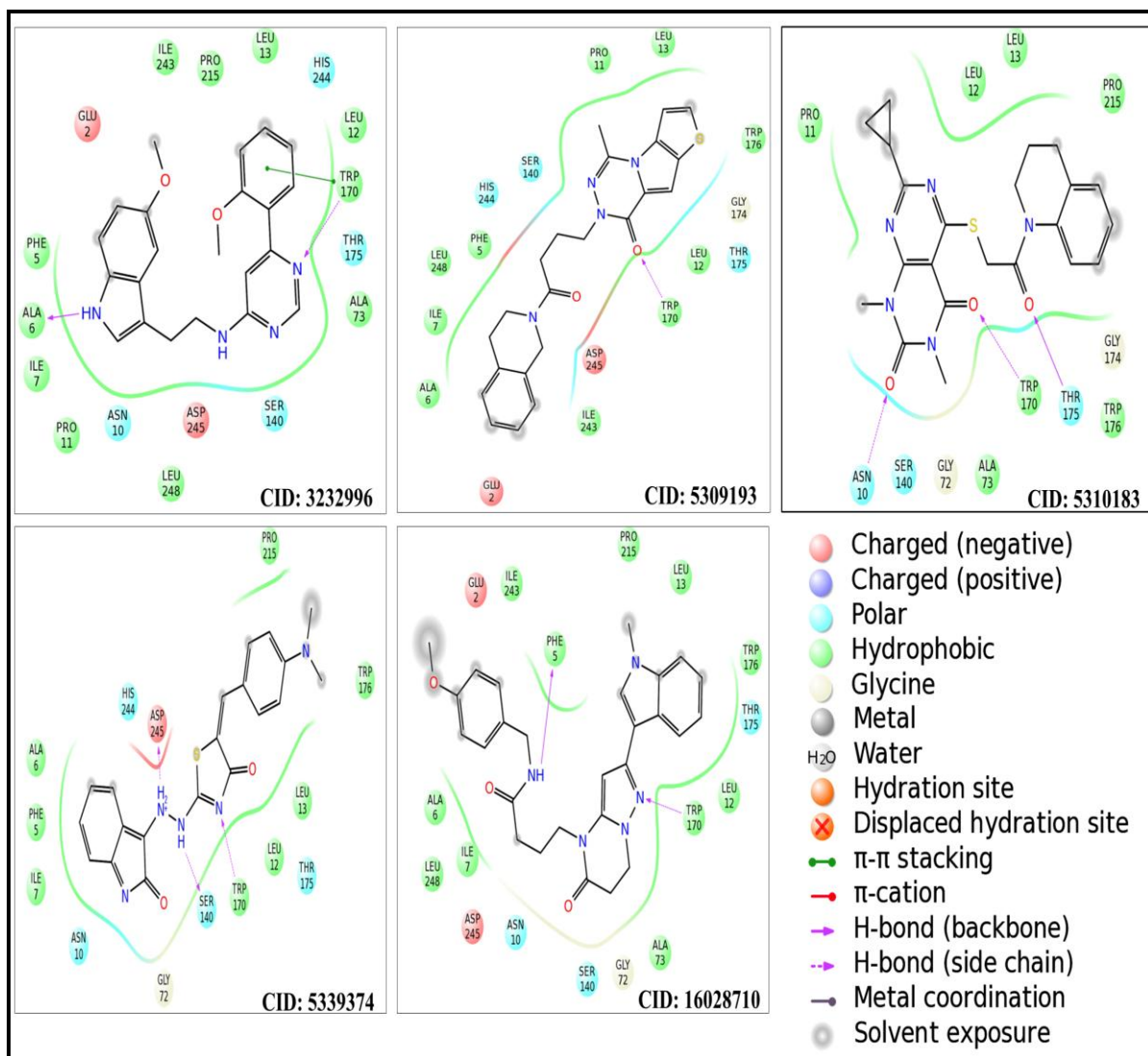
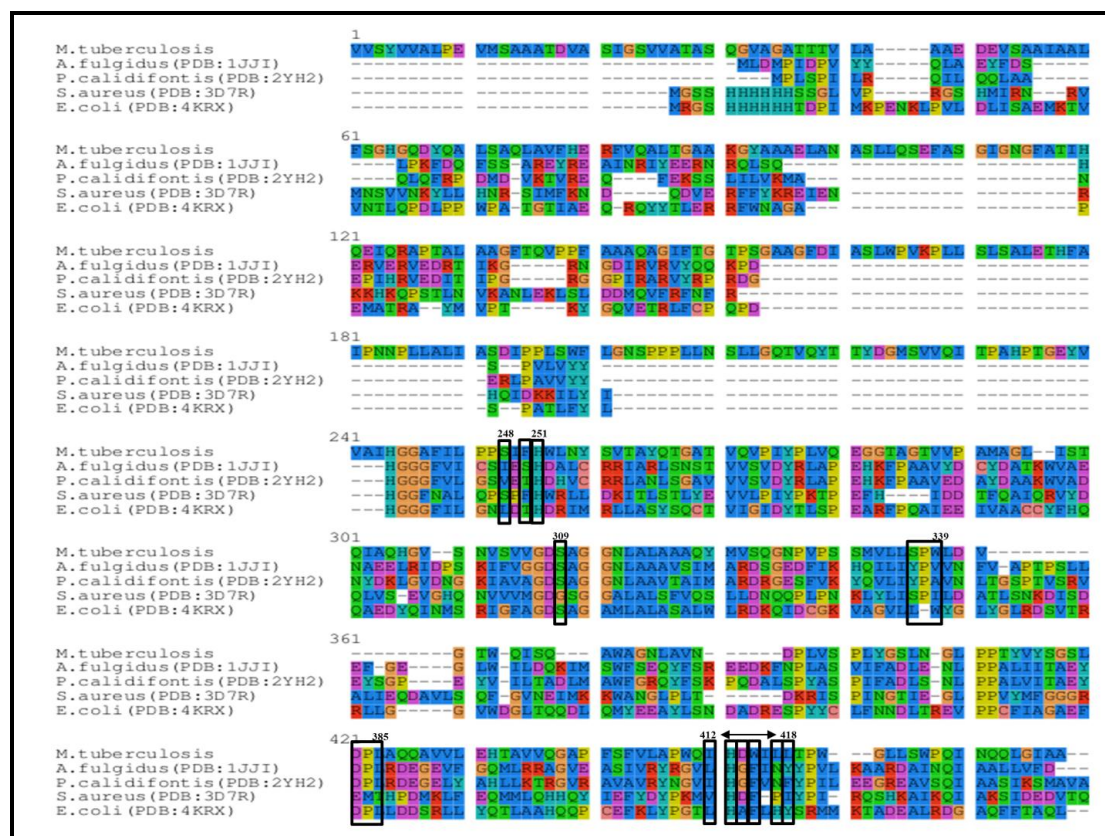


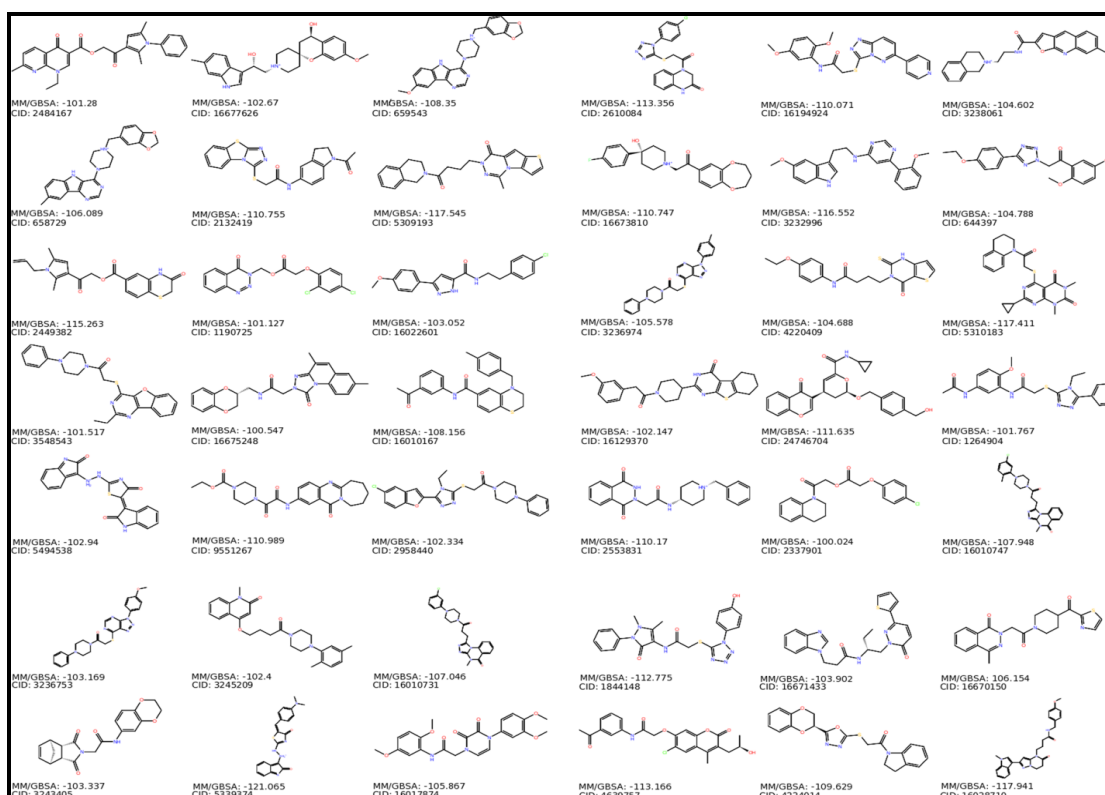
Fig. 9: The tree represents the scaffold analysis of 143 compounds by using Scaffold hunter. Dark circles indicate individual molecule whereas red circles indicate selected representative molecule from each cluster



**Fig. 10:** The docking of top five compounds with its compound ID inside the protein active site is shown. The active site residues are shown in sphere with different colour as per the amino acid type while type of interaction is also shown in different colour



Supplementary figure 1: The multiple sequence alignment of the selected five diverse species. The rectangular box indicates the conservation of sixteen active site residues in all species.



Supplementary figure 2: The 2D view of total 42 representative compounds from each cluster with respective PubChem ID and MM/GBSA score.

**Supplementary Table 1: The table represents the active and inactive molecules in cyan and pink colour. The average MM/GBSA score for the active and inactive molecules is -73.28 & -52.60. The average docking score for the active and inactive molecules is -7.0 and -6.8**

S. No.	Compound Name	Gscore (kcal/mol)	MM/GBSA (kcal/mol)	IC <sub>50</sub> value (μM)
1	8e	-6.929	-59.4	100
2	8j	-6.740	-59.1	100
3	8k	-6.774	-39.3	50
4	6a	-7.386	-88.8	25.00
5	8g	-6.001	-77.3	18.00
6	8b	-6.756	-59.6	12.50
7	8c	-8.043	-78.8	12.50
8	8d	-8.495	-60.0	9.25
9	8h	-7.073	-58.9	9.25
10	8f	-6.520	-70.1	8.25
11	8a	-7.676	-72.97	7.75
12	8i	-6.383	-56.5	5.13
13	Orlistat	-5.589	-109.8	1.50

**Supplementary Table 2: The PubChem CID, Glide docking score and MM/GBSA score of top five compounds**

S. No.	Compound ID	Glide score (kcal/mol)	MM/GBSA (kcal/mol)
1.	5339374	-7.46	-121.06
2.	16028710	-7.33	-117.94
3.	530193	-7.12	-117.45
4.	5310183	-7.50	-117.41
5.	3232996	-7.83	-116.55

## CONCLUSIONS

The present work was carried out to identify novel compounds that may inhibit LipY protein and play a significant role in *Mycobacterium tuberculosis* infection. In this study, we have used systematic virtual screening approach i.e. homology modeling, virtual screening and induced fit molecular docking approach for the identification of plausible hits. A total of 461,937 compounds from PubChem database were screened, and 42 compounds were identified. These new class of compounds can be used as novel antagonists against LipY receptor. Our model was able to discriminate between highly active and inactive molecules. Thus we can say that these set of molecules and the designed model can be used for virtual screening studies.

## ACKNOWLEDGEMENT

We are grateful to The Director, Institute of Life Sciences for the facilities and financial support. Suresh Satpati would like to acknowledge Department of Science and Technology (DST), Government of India for fellowship.

## REFERENCES

- Deng W., Li W., Zeng J., Zhao Q., Li C et al. Mycobacterium tuberculosis PPE Family Protein Rv1808 Manipulates Cytokines Profile via Co-Activation of MAPK and NF-κB Signaling Pathways. Cell Physiol. Biochem. 2014;33(2):273-288.
- Zaman K. Tuberculosis: A Global Health Problem. Journal of Health, Population and Nutrition. 2010;28(2):111–113.
- Roya AN., Ali M., Maliheh M., Mehdi M., Mahnaz Z. Factors associated with mortality in tuberculosis patients. J Res Med Sci. 2013;18(1):52–55.
- Gondrie P. Timebomb: The global epidemic of multi-drug resistant tuberculosis. Bulletin of the World Health Organization. 2002;80(6):514.
- Forrellad MA., Klepp IL., Gioffre A., Garcia JS., Morbidoni HR. et al, Virulence factors of the Mycobacterium tuberculosis complex. Virulence. 2013;4(1):3-66.
- Rajni, Rao N, Meena LS. Biosynthesis and Virulent Behavior of Lipids Produced by Mycobacterium tuberculosis: LAM and Cord Factor: An Overview. Biotechnol. Res. Int. 2011; 274693:7.
- Hett EC., Rubin EJ. Bacterial Growth and Cell Division: a Mycobacterial Perspective. Microbiol Mol Biol R. 2008;72(1):126-156.
- Liu J., Barry CE., Besra G.S., Nikaido H. Mycolic Acid Structure Determines the Fluidity of the Mycobacterial Cell Wall. J. Biol. Chem. 1996;271(47):29545-29551.
- Doroto MM., Katarzyna BP. Tuberculosis of the humerus. Pneumonol. Alergol. Pol. 2011;79(6):437-441.
- Jain A. Extra Pulmonary Tuberculosis: A Diagnostic Dilemma. Indian J. Clin. Biochem. 2011;26(3):269–273.
- Tania B., Bernhard R. Reactivation of

- Latent Tuberculosis Infection in TNF-Deficient Mice. *J. Immunol.* 2003;171(6):3110–3118.
12. Joanne LF., John C. Tuberculosis: Latency and Reactivation. *Infect Immun.* 2001;69(7):4195–4201.
  13. Marjanovic O., Miyata T., Goodridge A., Kendall LV., Riley LW. Mce2 operon mutant strain of *Mycobacterium tuberculosis* is attenuated in C57BL/6 mice. *Tuberculosis.* 2010;90(1):50-56.
  14. Vilchaze C., Hartman T., Weinrick B., Jacobs W. R. *Mycobacterium tuberculosis* is extraordinarily sensitive to killing by a vitamin C-induced Fenton reaction. *Nat. Commun.* 2013;4(1881).
  15. Smith I. *Mycobacterium tuberculosis* Pathogenesis and Molecular Determinants of Virulence. *Clin. Microbiol. Rev.* 2003;16(3):463-496.
  16. Akshata JS., Chakrabarthy A., Swapna R., Buggi S., Somashekhar M.. Adverse Drug Reactions in Management of Multi Drug Resistant in Tertiary Chest Institute. *JTR.* 2015;3(2):27-33.
  17. Chakraborty AK. Epidemiology of tuberculosis: Current status in India. *Indian J. Med. Res.* 2004;120(4):248-276.
  18. Sassetti CM., Boyd DH., Rubin EJ. Genes required for mycobacterial growth defined by high density mutagenesis. *Mol. Microbiol.* 2003;48(1):77-84.
  19. Bavishi A., Lin L., Choudhary M., Primm TP. Evolution of PE35 and PPE68 Gene Families in *Mycobacterium*: Roles of Horizontal Gene Transfer and Evolutionary Constraints. *JTR.* 2014;2:181-198.
  20. Mukhopadhyay S., Balaji KN. The PE and PPE proteins of *Mycobacterium tuberculosis*, *Tuberculosis.* 2011;91(5):441-447.
  21. Daleke MH., Cascioferro A., Punder KD., Ummels R., Abdallah AM. et al. Conserved Pro-Glu (PE) and Pro-Pro-Glu (PPE) Protein Domains Target LipY Lipases of Pathogenic *Mycobacteria* to the Cell Surface via the ESX-5 Pathway. *J. Biol. Chem.* 2011;286(21):19024-19034.
  22. Mishra KC., Chastellier CD., Narayana Y., Bifani P., Brown AK. et al. Functional Role of the PE Domain and Immunogenicity of the *Mycobacterium tuberculosis* Triacylglycerol Hydrolase LipY. *Infect. Immun.* 2008;76(1):127-140.
  23. Cotes K., Bakala N' Goma JC., Dhoubi R., Douchet I., Maurin D. et al. Lipolytic enzymes in *Mycobacterium tuberculosis*. *Appl. Microbiol. Biotechnol.* 2008;78(5):741-749.
  24. Saxena AK., Roy KK., Singh S., Vishnoi SP., Kumar A. et al. Identification and characterisation of small-molecule inhibitors of Rv3097c-encoded lipase (LipY) of *Mycobacterium tuberculosis* that selectively inhibit growth of bacilli in hypoxia. *Int. J. Antimicrob. Agents.* 2013;42(1):27-35.
  25. Singh VK., Srivastava M., Dasgupta A., Singh MP., Srivastava R. et al. Increased virulence of *Mycobacterium tuberculosis* H37Rv overexpressing LipY in a murine model. *Tuberculosis.* 2014;94(3):252-261.
  26. Point V., Malla RK., Diomande S., Martin BP., Delorme V., Carriere F., Canaan S., Rath N. P., Spilling CD., Cavalier JF. Synthesis and kinetic evaluation of cyclophostin and cyclophostins phosphonate analogs as selective and potent inhibitors of microbial lipases. *J. Med. Chem.* 2012;55(22):10204-19.
  27. Point V., Malla RK., Carriere F., Canaan S., Spilling CD., Cavalier J. Enantioselective Inhibition of Microbial Lipolytic Enzymes by Nonracemic Monocyclic Enolphosphonate Analogues of Cyclophostin. *J. Med. Chem.* 2013;56(11):4393-401.
  28. Delorme V., Diomande SV., Dedieu L., Cavalier J., Carriere F., Kremer L., Leclaire J., Fotiadu F., Canaan S. MmPPOX Inhibits *Mycobacterium tuberculosis* Lipolytic Enzymes Belonging to the Hormone-Sensitive Lipase Family and Alters *Mycobacterial* Growth. *PLoS ONE.* 2012;7(9):e46493.
  29. Ravindran SS., Rao SP., Cheng X., Shukla A., Cazenave-Gassiot A., Yao S. Q., Wenk MR. Targeting Lipid Esterases in *Mycobacteria* Grown Under Different Physiological Conditions Using Activity-based Profiling with Tetrahydrolipstatin (THL). *Mol Cell Proteomics.* 2014;13(2):435-448.
  30. Crellin PK., Vivian JP., Scoble J., Chow FM., West NP., Brammananth R., Proellocks NI., Shahine A., Le Nours J., Wilce MC., Britton WJ., Coppel RL., Rossjohn J., Beddoe T. Tetrahydrolipstatin inhibition, functional analyses, and three-dimensional structure of a lipase essential for mycobacterial viability. *J Biol Chem.* 2010;285(39):30050-60.
  31. Lewis DR., Liu DJ. Direct Measurement of Lipase Inhibition by Orlistat Using a Dissolution Linked In Vitro Assay. *Clini. Pharmacol. Biopharm.* 2012;1:1000103.
  32. Pemble CW., Johnson LC., Kridel SJ., Lowther WT. Crystal structure of the thioesterase domain of human fatty acid

- synthase inhibited by Orlistat. *Nat. Struct. Mol. Biol.* 2007;14(8):704-709.
33. Jorgensen WL., Maxwell DS., Rives JT. Development and Testing of the OPLS All-Atom Force Field on Conformational Energetics and Properties of Organic Liquids. *J. Am. Chem. Soc.* 1996;118(45):11225-11236.
  34. Altschul SF., Gish W., Miller W., Myers EW., Lipman DJ. Basic local alignment search tool, *J. Mol. Biol.* 1990;215(3):403-410.
  35. Pei J., Kim BH., Grishin NV. PROMALS3D: a tool for multiple protein sequence and structure alignments. *Nucleic Acids Res.* 2008;36(7):2295-2300.
  36. Eswar N., Webb B., Marti-Renom MA., Madhusudhan MS., Eramian D. et al. Comparative protein structure modeling with modeller. *Curr. Protoc. Bioinf.* 2006; 0.5:Unit-5.6.
  37. Lovell SC., Davis IW., Arendall WB., de Bakker PI., Word JM. et al. Structure validation by C $\alpha$  geometry: phi, psi and C $\beta$  deviation. *Proteins Struct. Funct. Genet.* 2003;50:437-450.
  38. Olsson MH., Sondergaard CR., Rostkowski M., Jensen JH. PROPKA3: Consistent Treatment of Internal and Surface Residues in Empirical pKa predictions. *J. Chem. Theor. Comput.* 2011;7(2):525-537.
  39. Sastry G.M., Adzhigirey M., Day T., Annabhimoju R., Sherman W. Protein and ligand preparation: Parameters, protocols, and influence on virtual screening enrichments. *J. Comput. Aid. Mol. Des.* 2011;27(3):221-234.
  40. Dalton J. A., Jackson R. M. Homology-Modelling Protein-Ligand Interactions: Allowing for Ligand-Induced Conformational Change. *J. Mol. Biol.* 2010;399(4):645-661.
  41. Evers A., Gohlke H., Klebe G. Ligand-supported Homology Modelling of Protein Binding-sites using Knowledge-based Potentials. *J. Mol. Biol.* 2003;334(2):327-345.
  42. Patny A., Desai P. V., Avery MA. Ligand-supported homology modeling of the human angiotensin II type 1 (AT1) receptor: Insights into the molecular determinants of telmisartan binding. *Proteins: Struct., Funct., Bioinf.* 2006;65(4):824-842.
  43. Sherman W., Day T., Jacobson MP., Friesner RA., Farid R. Novel Procedure for Modeling Ligand/Receptor Induced Fit Effects. *J. Med. Chem.* 2006;49(2):534-553.
  44. Hawkins PCD., Skillman AG., Warren GL., Ellingson BA., Stahl MT. Conformer Generation with OMEGA: Algorithm and Validation Using High Quality Structures from the Protein Databank and Cambridge Structural Database *J. Chem. Inf. Model.* 2010;50(4):572-584.
  45. Hawkins PCD., Skillman AG., Nicholls A. Comparison of Shape-Matching and Docking as Virtual Screening Tools. *J. Med. Chem.* 2007;50(1):74-82.
  46. Friesner RA., Banks JL., Murphy RB., Halgren TA., Klicic JJ et al. Glide: A New Approach for Rapid, Accurate Docking and Scoring. 1. Method and Assessment of Docking Accuracy. *J. Med. Chem.* 2004;47(7):1739-1749.
  47. Sirin S., Kumar R., Martinez C., Karmilowicz MJ., Ghosh P. et al. A Computational Approach to Enzyme Design: Predicting  $\omega$ -Aminotransferase Catalytic Activity Using Docking and MM-GBSA Scoring. *J. Chem. Inf. Model.* 2014;54(8):2334-2346.
  48. Klein K., Koch O., Kriege N., Mutzel P., Schafer T. Visual analysis of biological activity data with scaffold hunter. *Mol. Inf.* 2013;32(11-12):964-975.